AIAA JOURNAL
Vol. 36, No. 2, February 1998

Turbulence Modeling for Time-Dependent RANS and VLES: A Review

Charles G. Speziale*
Boston University, Boston, Massachusetts 02215

Reynolds stress models and traditional large-eddy simulations are reexamined with a view toward developing a combined methodology for the computation of complex turbulent flows. More specifically, an entirely new approach to time-dependent Reynolds-averaged Navier–Stokes (RANS) computations and very large-eddy simulations (VLES) is presented in which subgrid scale models are proposed that allow a direct numerical simulation (DNS) to go continuously to a RANS computation in the coarse mesh/infinite Reynolds number limit. In between these two limits, we have a large eddy simulation (LES) or VLES, depending on the level of resolution. The Reynolds stress model that is ultimately recovered in the coarse mesh/infinite Reynolds number limit has built in nonequilibrium features that make it suitable for time-dependent RANS. The fundamental technical issues associated with this new approach, which has the capability of bridging the gap between DNS, LES and RANS, are discussed in detail. Illustrative calculations are presented along with a discussion of the future implications of these results for the simulation of the turbulent flows of technological importance.

I. Introduction

PRACTICAL turbulent flows exhibit such a wide range of excited length- and timescales at high Reynolds numbers that direct simulations are not possible for the foreseeable future. This leaves Reynolds-averaged Navier–Stokes (RANS) computations and large-eddy simulations (LES) as the only realistic alternatives. Because of the inherent difficulties of developing reliable Reynolds stress models, it has been argued for a long time that LES, which at times has exhibited enormous potential, constitutes the preferred approach for the future. However, it must be said that traditional LES has never really lived up to its promise. Furthermore, because traditional LES is not possible at the extremely high Reynolds numbers that are often encountered in some technological applications, in those instances Reynolds stress models still remain the only viable approach. Thus, an LES capability must be developed that is formally tied to RANS, albeit a more general three-dimensional, time-dependent version, in the coarse mesh/infinite Reynolds number limit. This forms the motivation for the present paper.

Both traditional LES and Reynolds stress models will first be reviewed. It will be shown that the subgrid scale stress models that have been used in LES are deficient in that they correlate poorly with direct numerical simulations (DNS) and do not go to a state-of-the-art Reynolds stress model in the coarse mesh/infinite Reynolds number limit. In addition, it will be shown that most existing Reynolds stress models are only suitable for turbulent flows that are near equilibrium. The extension of these models to nonequilibrium turbulent flows will be systematically addressed. It will then be discussed how these results can be generalized to develop a new combined very large-eddy simulation (VLES) and time-dependent RANS capability that can have a significant impact on the computation of the complex turbulent flows of technological importance, an area that has recently been pursued by the author. The central points of the paper will be amplified by illustrative calculations and the basic technical issues associated with this new approach will be thoroughly discussed.

II. Review of LES

The foundation was laid for LES in the pioneering paper by Smagorinsky.[1] Because turbulence is, by its nature, three dimensional and time dependent, available computer capacities in the 1960s only allowed for extremely crude resolution under the circumstances. However, because the small scales of turbulence serve mainly to drain energy from the large scales through the cascade process, it was felt that their effect could be modeled in lieu of being resolved. Besides, the small scales of turbulence were believed to be more universal in character based on theoretical considerations dating from the time of Kolmogorov. Thus, it was argued that the large scales, which contain most of the energy and are known to be affected significantly by the flow configuration under consideration, should be computed directly while the small scales are modeled. These ideas have formed the basis for LES, which was first implemented into meteorological computations shortly after the groundbreaking work of Smagorinsky.[1]

As discussed, traditional LES is based on the filtered equations of motion. Any flow variable ϕ, in the fluid domain D, can be decomposed into a large-scale part and a small-scale part, respectively, as follows:

$$\phi = \bar{\phi} + \phi' \tag{1}$$

where

$$\bar{\phi} = \int_D G(\boldsymbol{x} - \boldsymbol{x}^*, \Delta)\phi(\boldsymbol{x}^*)\, \mathrm{d}^3x^* \tag{2}$$

constitutes the spatial filter of ϕ. In Eq. (2), Δ is the computational mesh size and G is a filter function for which

$$\int_D G(\boldsymbol{x} - \boldsymbol{x}^*, \Delta)\, \mathrm{d}^3x^* = 1 \tag{3}$$

The filter function G has usually been taken to be a Gaussian filter in infinite domains or a piecewise continuous distribution of bounded support in compact domains. (In the latter case, the simple box filter has been commonly used with finite difference methods.[2]) More specifically, the Gaussian filter is given by

$$G(\boldsymbol{x} - \boldsymbol{x}^*, \Delta) = \left(\frac{6}{\pi\Delta^2}\right)^{\frac{3}{2}} \exp\left(-6\frac{|\boldsymbol{x} - \boldsymbol{x}^*|^2}{\Delta^2}\right) \tag{4}$$

whereas the box filter, on a uniform mesh, takes the form

$$G(\boldsymbol{x} - \boldsymbol{x}^*, \Delta) = \begin{cases} \frac{1}{8}\Delta^3, & |x_i - x_i^*| \le \Delta \\ 0, & |x_i - x_i^*| > \Delta \end{cases} \tag{5}$$

for $i = 1, 2, 3$ (cf. Refs. 3 and 4). These features, along with the normalization constraint (3), guarantee that G becomes a Dirac delta sequence in the limit as $\Delta \to 0$,

Received April 13, 1997; presented as Paper 97-2051 at the AIAA 13th Computational Fluid Dynamics Conference, Snowmass Village, CO, June 29–July 2, 1997; revision received Sept. 18, 1997; accepted for publication Oct. 6, 1997.

*Professor, Aerospace and Mechanical Engineering Department. Member AIAA.

$$\lim_{\Delta \to 0} \int_D G(\boldsymbol{x} - \boldsymbol{x}^*, \Delta)\phi(\boldsymbol{x}^*)\, \mathrm{d}^3 x^*$$

$$= \int_D \delta(\boldsymbol{x} - \boldsymbol{x}^*)\phi(\boldsymbol{x}^*)\, \mathrm{d}^3 x^* \equiv \phi(\boldsymbol{x}) \tag{6}$$

where $\delta(\boldsymbol{x}-\boldsymbol{x}^*)$ is the Dirac delta function. (Thus, direct simulations are recovered in the fine mesh limit.) As a result of the Riemann–Lebesgue theorem, Eq. (2) substantially reduces the amplitude of the high wave number Fourier components in space of any flow variable ϕ. (Consequently, $\bar{\phi}$ constitutes the large-scale part of ϕ.) Unlike with traditional Reynolds averages,

$$\bar{\bar{\phi}} \neq \bar{\phi}, \qquad \bar{\phi}' \neq 0 \tag{7}$$

in general. The only major exception is the sharp Fourier cutoff filter, which renders $\bar{\phi}' = 0$ because it annihilates all Fourier components above some critical wave number; in physical space it is given by

$$G(\boldsymbol{x} - \boldsymbol{x}^*, \Delta) = \frac{1}{(\pi\Delta)^3} \prod_{i=1}^{3} \frac{\sin\left[\left(x_i - x_i^*\right)/\Delta\right]}{\left(x_i - x_i^*\right)/\Delta} \tag{8}$$

Because spectral methods are based on a representation consisting of a finite number of Fourier modes, they are actually implicitly invoking such a filter. For the common choice of filters just discussed, the filtering process commutes with both time and spatial derivatives, i.e.,

$$\frac{\overline{\partial\phi}}{\partial t} = \frac{\partial\bar{\phi}}{\partial t}, \qquad \frac{\overline{\partial\phi}}{\partial x_k} = \frac{\partial\bar{\phi}}{\partial x_k} \tag{9}$$

For incompressible turbulent flows, a straightforward filtering of the Navier–Stokes equations yields

$$\frac{\partial\bar{u}_i}{\partial t} + \bar{u}_j\frac{\partial\bar{u}_i}{\partial x_j} = -\frac{\partial\bar{p}}{\partial x_i} + \nu\nabla^2\bar{u}_i - \frac{\partial\tau_{ij}}{\partial x_j} \tag{10}$$

where $\bar{u}_i$ is the filtered velocity, $\bar{p}$ is the filtered kinematic pressure, ν is the kinematic viscosity, and τ_{ij} is the subgrid-scale stress tensor ($\tau_{ij} \to 0$ as $\Delta \to 0$). Of course, the incompressible continuity equation requires that $\partial\bar{u}_i/\partial x_i = 0$. The full form of the subgrid-scale stress tensor is given by

$$\tau_{ij} = L_{ij} + C_{ij} + R_{ij} \tag{11}$$

where

$$L_{ij} \equiv \overline{\bar{u}_i\bar{u}_j} - \bar{u}_i\bar{u}_j \tag{12}$$

$$C_{ij} \equiv \overline{\bar{u}_i u_j' + u_i'\bar{u}_j} \tag{13}$$

$$R_{ij} \equiv \overline{u_i' u_j'} \tag{14}$$

are, respectively, the Leonard stresses, subgrid-scale cross stresses, and subgrid-scale Reynolds stresses.[3]

Smagorinsky[1] proposed the first subgrid-scale stress model, as discussed earlier. The Smagorinsky model constitutes an eddy viscosity model that takes the form

$$\tau_{ij} = -2C_s\Delta^2(2\bar{S}_{kl}\bar{S}_{kl})^{\frac{1}{2}}\bar{S}_{ij} \tag{15}$$

where

$$\bar{S}_{ij} = \frac{1}{2}\left(\frac{\partial\bar{u}_i}{\partial x_j} + \frac{\partial\bar{u}_j}{\partial x_i}\right)$$

is the filtered rate of strain tensor and C_s is a constant that bears his name, i.e., the Smagorinsky constant, which in earlier treatments of the subject was defined in terms of $\sqrt{C_s}$. Here, note that, for consistency, Eq. (15) only applies to the deviatoric part of τ_{ij}. The Smagorinsky model is a tensorially invariant generalization of the mixing length type representation that can only be expected to apply if there is a separation of scales. Because practical LES has always required that a significant fraction of the turbulent kinetic energy is left unresolved, there is no clear-cut separation of scales between the resolved and unresolved scales. Hence, it is not surprising that subsequent studies showed that the Smagorinsky model correlates poorly with the results of DNS even for simple test cases such as isotropic turbulence.[5,6] The successes that it has had are probably tied to the fact that, with the appropriate choice of the constant C_s, the Smagorinsky model provides roughly the correct amount of dissipation to approximately account for the energy cascade to the scales that are not resolved. This is supported by the fact that different flows have tended to require a different value of the Smagorinsky constant. Values for C_s have varied from approximately 0.005–0.05, where the lower values have been used for channel flow and the higher values have been used for isotropic turbulence. As alluded to before, the Smagorinsky model was used early on, with success, in meteorological computations. A few years later, Deardorff[2] reported the first LES of a practical engineering flow, namely, turbulent channel flow. That study was conducted with finite difference techniques using the Smagorinsky model based on a box filter. However, limitations in computer capacity at that time, along with the numerical errors introduced by second-order accurate finite difference techniques, severely restricted the range of applicability of the results (as well as the reliability, except at very low-turbulence Reynolds numbers, at best).

During the time frame of the late 1970s and early 1980s, some further progress was made on the LES of turbulence using spectral methods (see Ref. 7 for a more detailed review of this work). A major thrust was undertaken on subgrid-scale modeling in an effort to develop models that transcend the Smagorinsky model. The Smagorinsky model can be thought of as combining the Reynolds averaging assumption, given by

$$L_{ij} + C_{ij} = 0 \tag{16}$$

with a mixing-length-based eddy viscosity model for the Reynolds subgrid-scale stress tensor wherein the mixing length is taken to be proportional to the computational mesh size Δ as given in Eq. (15). Clark et al.[5] tested a variety of possible subgrid-scale models and developed a new model for the Leonard[3] and subgrid-scale cross stresses, via a Taylor expansion, while maintaining the Smagorinsky model for the subgrid-scale Reynolds stresses. The Clark et al.[5] proposal takes the form

$$L_{ij} + C_{ij} = \frac{1}{12}\Delta^2\frac{\partial\bar{u}_i}{\partial x_k}\frac{\partial\bar{u}_j}{\partial x_k} \tag{17}$$

$$R_{ij} = -2C_s\Delta^2(2\bar{S}_{kl}\bar{S}_{kl})^{\frac{1}{2}}\bar{S}_{ij} \tag{18}$$

where Eq. (17), which is dispersive in character and accounts for backscatter effects, is formally obtained from a second-order accurate Taylor expansion. [Again, for consistency, Eq. (18) only applies to the deviatoric part of R_{ij}.]

Motivated by the earlier work of Leslie and co-workers, Biringen and Reynolds[8] and Moin and Kim[9] began to calculate the Leonard stresses directly. From Eq. (12) it is clear that, once $\bar{u}_i$ is known, L_{ij} can be calculated directly. When spectral methods are used, it is relatively straightforward to do so by means of a standard convolution theorem. (In physical space, however, this is more difficult to do.) Both Biringen and Reynolds[8] and Moin and Kim[9] calculated the Leonard stresses (L_{ij}) directly, whereas they applied the Smagorinsky model (15) to $C_{ij} + R_{ij}$, instead. A few years later, Speziale[10] showed that such an approach was not Galilean invariant. Whereas the Reynolds subgrid-scale stress tensor (R_{ij}) and the sum of the Leonard and subgrid scale cross stresses ($L_{ij} + C_{ij}$) are Galilean invariant, neither L_{ij} nor C_{ij} are invariant by themselves. Hence, modeling $C_{ij} + R_{ij}$ by the Smagorinsky model is inconsistent and destroys the Galilean invariance of the subgrid-scale stress tensor. Thus, the filtered equations of motion solved by both Biringen and Reynolds[8] and Moin and Kim[9] were not Galilean invariant and, as such, violated Newton's first law. Furthermore, the subgrid-scale cross stresses largely account for backscatter effects, i.e., a reverse cascade from the small to the large scales, and, as such, are dispersive in character. Modeling them with the Smagorinsky model, which is purely dissipative, is not physically consistent. Bardina et al.[11] later developed the scale similarity model for C_{ij}

in an alternative effort to improve on the Smagorinsky model by calculating the Leonard stresses directly. Their proposal, which is referred to as the linear combination model,[11] is given by

$$C_{ij} = c_r(\bar{u}_i\bar{u}_j - \bar{\bar{u}}_i\bar{\bar{u}}_j) \tag{19}$$

$$R_{ij} = -2C_s\Delta^2(2\bar{S}_{kl}\bar{S}_{kl})^{\frac{1}{2}}\bar{S}_{ij} \tag{20}$$

where the Leonard stresses L_{ij} are calculated directly via a convolution. Based on a calibration employing DNS results from homogeneous turbulence, Bardina et al.[11] arrived at a value of the constant $c_r = 1.1$. Speziale[10] and Reynolds later independently showed that the scale similarity model is Galilean invariant if and only if

$$c_r = 1 \tag{21}$$

Bardina et al.[11] conducted LES of a range of benchmark homogeneous turbulent flows using the linear combination model, with moderate success. Piomelli et al.,[12] building on the earlier groundbreaking work of Moin and Kim,[9] conducted LES of turbulent channel flow that was quite successful in overcoming many of the earlier problems already discussed. Early on, Schumann[13] investigated the use of transport models for the subgrid-scale stress tensor, as well as algebraic models obtained therefrom, and later made contributions to the LES of geophysical flows.[14] Speziale et al.[15] developed a variable density extension of the linear combination model suitable for the LES of compressible turbulence. Then, Erlebacher et al.[6,16] published the first LES of a high-speed compressible turbulent flow, namely, compressible isotropic turbulence.

A resurgence of interest in LES has developed during the past few years. An effort has been directed to resolve two of the major lingering problems with LES: 1) the inability of subgrid scale models to respond to changes in the local state of the flow, causing the need to make ad hoc adjustments in the constants; and 2) the generally poor correlation of subgrid-scale models with DNS at lower turbulence Reynolds numbers, even for simple benchmark cases.

In regard to point 1, turbulent channel flow, isotropic turbulence, and more general homogeneously strained turbulent flows all require different values of the Smagorinsky constant that can differ by more than a factor of two, even when given in its traditional form of $\sqrt{C_s}$. Furthermore, Van Driest wall damping has been needed, which is empirical in nature and does not apply to general wall-bounded turbulent flows, particularly to those in complex geometries or with flow separation. Then, as far as point 2 is concerned, even for the simple case of isotropic turbulence, the Smagorinsky model only correlates at the 50% level, an extremely poor result. Note, for example, that the correlation between the functions $y = x$ and $y = e^{-x}$ on the interval [0, 1] is more than 50% despite the fact that they are qualitatively different functions. (One is monotonically increasing, whereas the other is monotonically decreasing.)

As alluded to earlier, the only reason to believe that the Smagorinsky model is successful in these cases is probably because it dissipates enough energy to roughly account for the cascade of energy to the scales that are left unresolved. With the desire to eliminate these problems, the dynamic subgrid-scale model was recently developed.[17] In the dynamic subgrid-scale model, a test filter is introduced in addition to the grid filter, discussed earlier, in Eq. (2). A variable Smagorinsky coefficient is then derived that depends on the local filtered rate-of-strain tensor, as well as on the resolved turbulent stresses. The Smagorinsky coefficient then has the capability, in principle, of adapting automatically to the local state of the flow. Whereas the dynamic subgrid-scale model does contain many interesting new ideas, it, unfortunately, further exacerbates the problem of contamination of the large scales by filtering and is not suitable for turbulent flows in complex geometries where the effect of the filter is never known with certainty and defiltering is not possible with any reliability. Furthermore, the dynamic subgrid-scale model suffers from the same deficiency as the older subgrid-scale models because in the coarse mesh and infinite-Reynolds-number limit, a state-of-the-art Reynolds stress model is not recovered. (The Smagorinsky model goes to a badly calibrated mixing length model in the coarse mesh limit.) In the opinion of the author, future subgrid-scale models should be theoretically based on a filter that does not significantly contaminate the large scales insofar as the model calibration is concerned, with the understanding that for complex turbulent flows one will never know precisely the effect of the filter. In this manner, the issue of defiltering is completely avoided because it can never be done reliably anyhow. (This is equivalent to solving a Fredholm integral equation of the first kind, which is mathematically ill-posed.[18]) Then, even more importantly, a state-of-the-art Reynolds stress model should be recovered in the coarse mesh/infinite Reynolds number limit. (The dynamic subgrid-scale model fails on both counts.) The author has recently proposed just such a new approach to LES in a major effort to bridge the gap between LES and RANS to develop a more practical LES capability. Before discussing this new approach, Reynolds stress models will first be reviewed.

III. Review of Reynolds Stress Models

Incompressible turbulent flows are again considered, where the velocity u_i and kinematic pressure p can be decomposed into ensemble mean and fluctuating parts as follows:

$$u_i = \bar{u}_i + u_i', \qquad p = \bar{p} + p' \tag{22}$$

where an overbar is an ensemble mean. (Here, time averages can be used in statistically steady turbulent flows, whereas spatial averages can be used in homogeneous turbulent flows.) The mean velocity and pressure are solutions of the Reynolds-averaged Navier–Stokes and continuity equations, which are given by[19]

$$\frac{\partial\bar{u}_i}{\partial t} + \bar{u}_j\frac{\partial\bar{u}_i}{\partial x_j} = -\frac{\partial\bar{p}}{\partial x_i} + \nu\nabla^2\bar{u}_i - \frac{\partial\tau_{ij}}{\partial x_j} \tag{23}$$

$$\frac{\partial\bar{u}_i}{\partial x_i} = 0 \tag{24}$$

where $\tau_{ij} \equiv \overline{u_i'u_j'}$ now is the Reynolds stress tensor and ν the kinematic viscosity. The Reynolds stress tensor is a solution of the transport equation[19]

$$\frac{\mathrm{D}\tau_{ij}}{\mathrm{D}t} = -\tau_{ik}\frac{\partial\bar{u}_j}{\partial x_k} - \tau_{jk}\frac{\partial\bar{u}_i}{\partial x_k} + \Pi_{ij} - \varepsilon_{ij} + \mathcal{D}_{ij}^T + \nu\nabla^2\tau_{ij} \tag{25}$$

where $D/Dt \equiv \partial/\partial t + \bar{\boldsymbol{u}}\cdot\nabla$ is the mean convective derivative and

$$\Pi_{ij} = \overline{p'\left(\frac{\partial u_i'}{\partial x_j} + \frac{\partial u_j'}{\partial x_i}\right)}, \qquad \varepsilon_{ij} = 2\nu\overline{\left(\frac{\partial u_i'}{\partial x_k}\frac{\partial u_j'}{\partial x_k}\right)} \tag{26}$$

$$\mathcal{D}_{ij}^T = -\frac{\partial}{\partial x_k}(\overline{u_i'u_j'u_k'} + \overline{p'u_i'}\delta_{jk} + \overline{p'u_j'}\delta_{ik}) \tag{27}$$

are, respectively, the pressure-strain correlation, the dissipation rate tensor, and the turbulent diffusion terms. Equation (25) is obtained by taking a second moment of the fluctuating Navier–Stokes equation.

Second-order closures are based on the solution of a modeled form of the Reynolds stress transport equation given in Eq. (25). On the other hand, two-equation models, such as the K–ε model of Launder and Spalding,[20] have typically been based on an empirical eddy viscosity representation for the Reynolds stress tensor that is solved with modeled transport equations for the turbulent kinetic energy K and the turbulent dissipation rate ε. Here, it will be shown that two-equation models formally follow from second-order closures in the limit of homogeneous turbulence in equilibrium. However, the two-equation models that are obtained in this way constitute anisotropic eddy viscosity models with strain-dependent coefficients. The eddy viscosity representation is recovered for the turbulent shear stress, in the thin shear flow limit, under equilibrium conditions.

Homogeneous turbulence in equilibrium, as well as local regions of inhomogeneous turbulent flows where there is a production-equals-dissipation equilibrium, satisfies the constraints

$$\frac{\mathrm{D}b_{ij}}{\mathrm{D}t} = 0 \tag{28}$$

$$\mathcal{D}_{ij}^T + \nu\nabla^2\tau_{ij} = 0 \tag{29}$$

where

$$b_{ij} = \frac{\tau_{ij} - \frac{2}{3}K\delta_{ij}}{2K} \tag{30}$$

is the Reynolds stress anisotropy tensor. ($K \equiv \frac{1}{2}\overline{u_i' u_i'}$ is the turbulent kinetic energy.) In physical terms, this is an equilibrium for which convective and transport effects can be neglected; it is the basic equilibrium hypothesis used in the derivation of algebraic stress models (ASMs). However, it is only globally valid for homogeneous turbulent flows that are in equilibrium.

It follows directly from Eqs. (28) and (30) that

$$\frac{D\tau_{ij}}{Dt} = \frac{\tau_{ij}}{K}\frac{DK}{Dt} \tag{31}$$

and, hence, by making use of the contraction of Eqs. (25) and (29), it can be shown that

$$\frac{D\tau_{ij}}{Dt} = (\mathcal{P} - \varepsilon)\frac{\tau_{ij}}{K} \tag{32}$$

where $\mathcal{P} \equiv -\tau_{ij}\partial\bar{u}_i/\partial x_j$ is the turbulence production and $\varepsilon \equiv \frac{1}{2}\varepsilon_{ii}$ is the (scalar) turbulent dissipation rate. The substitution of Eqs. (29) and (32) into Eq. (25) yields the following equilibrium form of the Reynolds stress transport equation:

$$(\mathcal{P} - \varepsilon)\frac{\tau_{ij}}{K} = -\tau_{ik}\frac{\partial\bar{u}_j}{\partial x_k} - \tau_{jk}\frac{\partial\bar{u}_i}{\partial x_k} + \Pi_{ij} - \frac{2}{3}\varepsilon\delta_{ij} \tag{33}$$

where the Kolmogorov assumption of local isotropy,[19] given by

$$\varepsilon_{ij} = \tfrac{2}{3}\varepsilon\delta_{ij} \tag{34}$$

for high Reynolds number turbulence, has also been applied. By making use of Eq. (30), we can rearrange Eq. (33) into the alternative form in terms of the Reynolds stress anisotropy tensor

$$(\mathcal{P} - \varepsilon)b_{ij} = -\tfrac{2}{3}K\bar{S}_{ij} - K\left(b_{ik}\bar{S}_{jk} + b_{jk}\bar{S}_{ik} - \tfrac{2}{3}b_{mn}\bar{S}_{mn}\delta_{ij}\right) + K(b_{ik}\bar{\omega}_{jk} + b_{jk}\bar{\omega}_{ik}) + \tfrac{1}{2}\Pi_{ij} \tag{35}$$

where

$$\bar{S}_{ij} = \frac{1}{2}\left(\frac{\partial\bar{u}_i}{\partial x_j} + \frac{\partial\bar{u}_j}{\partial x_i}\right) \tag{36}$$

$$\bar{\omega}_{ij} = \frac{1}{2}\left(\frac{\partial\bar{u}_i}{\partial x_j} - \frac{\partial\bar{u}_j}{\partial x_i}\right) \tag{37}$$

are the mean rate of strain and mean vorticity tensors.

In virtually all of the commonly used second-order closure models based on Eq. (25), Π_{ij} is modeled in the general form[21,22]

$$\Pi_{ij} = \varepsilon\mathcal{A}_{ij}(\boldsymbol{b}) + K\mathcal{M}_{ijkl}(\boldsymbol{b})\frac{\partial\bar{u}_k}{\partial x_l} \tag{38}$$

which is formally valid for homogeneous turbulent flows near equilibrium. The substitution of Eq. (38) into Eq. (35) yields a closed system of algebraic equations for the determination of the Reynolds stress anisotropy tensor in terms of the mean velocity gradients. This constitutes the general form of the traditional ASMs of turbulence.[23] These traditional ASMs are implicit because the Reynolds stress tensor appears on both sides of the equation.

It has been shown that the most general form of Eq. (38) for two-dimensional mean turbulent flows in equilibrium reduces to[22,24]

$$\Pi_{ij} = -C_1\varepsilon b_{ij} + C_2K\bar{S}_{ij} + C_3K\left(b_{ik}\bar{S}_{jk} + b_{jk}\bar{S}_{ik} - \tfrac{2}{3}b_{mn}\bar{S}_{mn}\delta_{ij}\right) + C_4K(b_{ik}\bar{\omega}_{jk} + b_{jk}\bar{\omega}_{ik}) \tag{39}$$

where the quadratic return term is neglected, which is typically small since it is directly proportional to $\varepsilon b_{ik}b_{kj}$, and where $C_1 - C_4$ are constants. Speziale et al.[24] showed that a range of strained two-dimensional homogeneous turbulent flows near equilibrium can be collapsed using Eq. (39) with the constants $C_1 = 6.80$, $C_2 = 0.36$, $C_3 = 1.25$, and $C_4 = 0.40$. Out of equilibrium, the first two coefficients are functions of the ratio of production to dissipation $\mathcal{P}/\varepsilon$ and the second invariant II_b of b_{ij}, which makes the Ref. 24 model weakly nonlinear. [These coefficients become constants in equilibrium yielding a linear rapid pressure–strain model,[24] which is needed for a closed-form analytical solution to be obtainable from Eq. (35).] This will be discussed later.

The direct substitution of Eq. (39) into Eq. (35) yields the equation

$$b_{ij} = \tfrac{1}{2}g\tau\left[\left(C_2 - \tfrac{4}{3}\right)\bar{S}_{ij} + (C_3 - 2)\left(b_{ik}\bar{S}_{jk} + b_{jk}\bar{S}_{ik} - \tfrac{2}{3}b_{mn}\bar{S}_{mn}\delta_{ij}\right) + (C_4 - 2)(b_{ik}\bar{\omega}_{jk} + b_{jk}\bar{\omega}_{ik})\right] \tag{40}$$

where

$$g = [(C_1/2) + (\mathcal{P}/\varepsilon) - 1]^{-1} \tag{41}$$

and $\tau \equiv K/\varepsilon$ is the turbulent timescale.[25,26]

For homogeneous turbulence, the turbulent kinetic energy K and dissipation rate ε are solutions of the transport equations

$$\dot{K} = \mathcal{P} - \varepsilon \tag{42}$$

$$\dot{\varepsilon} = C_{\varepsilon 1}(\varepsilon/K)\mathcal{P} - C_{\varepsilon 2}(\varepsilon^2/K) \tag{43}$$

where $C_{\varepsilon 1}$ and $C_{\varepsilon 2}$ are constants that most recently have assumed the values of 1.44 and 1.83, respectively. Here, the first equation is exact, whereas the second equation follows from plausible modeling assumptions for homogeneous turbulence near equilibrium.[22] Equations (42) and (43) yield the following equilibrium solution for the ratio of production to dissipation:

$$\frac{\mathcal{P}}{\varepsilon} = \frac{C_{\varepsilon 2} - 1}{C_{\varepsilon 1} - 1} \tag{44}$$

If we introduce the dimensionless, rescaled variables[26]

$$S_{ij}^* = \tfrac{1}{2}g\tau(2 - C_3)\bar{S}_{ij}, \qquad \omega_{ij}^* = \tfrac{1}{2}g\tau(2 - C_4)\bar{\omega}_{ij} \tag{45}$$

$$b_{ij}^* = \left(\frac{C_3 - 2}{C_2 - \frac{4}{3}}\right)b_{ij} \tag{46}$$

then Eq. (40) reduces to the simpler form

$$b_{ij}^* = -S_{ij}^* - \left(b_{ik}^*S_{jk}^* + b_{jk}^*S_{ik}^* - \tfrac{2}{3}b_{kl}^*S_{kl}^*\delta_{ij}\right) + b_{ik}^*\omega_{kj}^* + b_{jk}^*\omega_{ki}^* \tag{47}$$

which is linear in b_{ij} by virtue of Eq. (44).

The explicit solution to Eq. (47) for two-dimensional mean turbulent flows, obtained by integrity bases methods, renders the closed-form expression[25,26]

$$b_{ij}^* = -\frac{3}{3 - 2\eta^2 + 6\xi^2}\left[S_{ij}^* + S_{ik}^*\omega_{kj}^* + S_{jk}^*\omega_{ki}^* - 2\left(S_{ik}^*S_{kj}^* - \tfrac{1}{3}S_{k\ell}^*S_{k\ell}^*\delta_{ij}\right)\right] \tag{48}$$

where

$$\eta = \left(S_{ij}^*S_{ij}^*\right)^{\frac{1}{2}}, \qquad \xi = \left(\omega_{ij}^*\,\omega_{ij}^*\right)^{\frac{1}{2}} \tag{49}$$

In more familiar terms, this expression is equivalent to the form

$$\tau_{ij} = \frac{2}{3}K\delta_{ij} - \frac{3}{3 - 2\eta^2 + 6\xi^2}\left[\alpha_1\frac{K^2}{\varepsilon}\bar{S}_{ij} + \alpha_2\frac{K^3}{\varepsilon^2}(\bar{S}_{ik}\bar{\omega}_{kj} + \bar{S}_{jk}\bar{\omega}_{ki}) - \alpha_3\frac{K^3}{\varepsilon^2}\left(\bar{S}_{ik}\bar{S}_{kj} - \frac{1}{3}\bar{S}_{k\ell}\bar{S}_{k\ell}\delta_{ij}\right)\right] \tag{50}$$

where α_1, α_2, and α_3 are constants related to the coefficients $C_1 - C_4$ and g (see Ref. 26 for more details). By virtue of the homogeneous equilibrium assumption, which renders the constant value for $\mathcal{P}/\varepsilon$ given in Eq. (44), Eq. (48) is fully explicit. When this expression is applied to inhomogeneous turbulent flows that are out

of equilibrium, which is typically done based on a local, homogeneous equilibrium assumption, a singularity can occur through the vanishing of the denominator $(3 - 2\eta^2 + 6\xi^2)$ in Eq. (48). Gatski and Speziale[26] introduced the simple regularization

$$\frac{3}{3 - 2\eta^2 + 6\xi^2} \approx \frac{3(1 + \eta^2)}{3 + \eta^2 + 6\xi^2\eta^2 + 6\xi^2} \tag{51}$$

which is obtained by a Taylor expansion that is a systematic approximation for η and ξ sufficiently less than one. For turbulent flows that are near equilibrium, where Eq. (48) is formally valid and η and $\xi < 1$, this approximation yields results that are indistinguishable from the original expression $3/(3 - 2\eta^2 + 6\xi^2)$, all within the framework of a model that is regular and computable for all values of η and ξ. More recently, Speziale and Xu[27] conducted a formal Padé approximation of the coefficient $3/(3 - 2\eta^2 + 6\xi^2)$ that regularizes while building in some limited agreement with the rapid distortion theory (RDT) solution for homogeneous shear flow that is strongly sheared where η and $\xi \gg 1$. Abid et al.[28] conducted a heuristic Padé approximation that takes the alternative, pragmatic view of maintaining a finite lower bound for the eddy viscosity for numerical robustness. [On the other hand, Eq. (51) yields a vanishing eddy viscosity as η and $\xi \to \infty$, which can be numerically destabilizing.] These points will be discussed in more detail in Secs. IV and V.

Equation (48), with a regularized expression for the strain-dependent coefficient $3/(3-2\eta^2+6\xi^2)$, constitutes the general form of the regularized, explicit ASMs. They are in the form of anisotropic eddy viscosity models with strain-dependent coefficients. These models are the explicit solution to the traditional implicit ASMs such as that due to Rodi.[23] These latter implicit models can give rise to multiple solutions or singularities (when solved iteratively) and, hence, should be abandoned in the future.[29]

In rotating frames, Coriolis terms must be added to the right-hand side (RHS) of the Reynolds stress transport equation (25). Gatski and Speziale[26] showed that this analysis can exactly account for such noninertial effects in rotating frames if the extended definition of ω_{ij}^* is used:

$$\omega_{ij}^{*E} = \tfrac{1}{2}g(K/\varepsilon)(2 - C_4)[\bar{\omega}_{ij} + (C_4 - 4)/(C_4 - 2)e_{mji}\Omega_m]$$

where Ω_m is the angular velocity of the reference frame and e_{ijk} is the permutation tensor. (In the limit as $\Omega_m \to 0$ we recover ω_{ij}^*.)

If we have a separation of scales, then η and $\xi \ll 1$ and, in the linear limit, we recover the eddy viscosity model

$$\tau_{ij} = \tfrac{2}{3}K\delta_{ij} - 2C_\mu(K^2/\varepsilon)\bar{S}_{ij} \tag{52}$$

which forms the basis for the standard K–ε model of Launder and Spalding,[20] where C_μ is a constant. However, in practical turbulent flows we do not have a separation of scales; η and ξ are of $\mathcal{O}(1)$. Nonetheless, for two-dimensional turbulent shear flows in a production-equals-dissipation equilibrium, the model of Gatski and Speziale[26] given in Eq. (50) yields

$$\tau_{xy} = -C_\mu \frac{K^2}{\varepsilon}\frac{\partial \bar{u}_x}{\partial y} \tag{53}$$

with

$$C_\mu \approx 0.094 \tag{54}$$

which is remarkably close to the value of $C_\mu = 0.09$ used in the standard K–ε model.[20]

For inhomogeneous turbulence, this regularized algebraic representation of the Reynolds stress tensor is solved with modeled transport equations for the turbulent kinetic energy K and dissipation rate ε. For weakly inhomogeneous turbulent flows that are near equilibrium, we can extend the K and ε transport equations given in Eqs. (42) and (43) by the addition of gradient transport terms that are obtained by a formal expansion technique. After replacing the time derivative by the mean convective derivative, these resulting transport equations take the form

$$\frac{\partial K}{\partial t} + \bar{\boldsymbol{u}} \cdot \nabla K = \mathcal{P} - \varepsilon + \frac{\partial}{\partial x_i}\left(\frac{\nu_T}{\sigma_k}\frac{\partial K}{\partial x_i}\right) \tag{55}$$

$$\frac{\partial \varepsilon}{\partial t} + \bar{\boldsymbol{u}} \cdot \nabla \varepsilon = C_{\varepsilon 1}\frac{\varepsilon}{K}\mathcal{P} - C_{\varepsilon 2}\frac{\varepsilon^2}{K} + \frac{\partial}{\partial x_i}\left(\frac{\nu_T}{\sigma_\varepsilon}\frac{\partial \varepsilon}{\partial x_i}\right) \tag{56}$$

where σ_k and σ_ε are constants that typically assume the values of 1.0 and 1.3, respectively, and $\nu_T \equiv C_\mu K^2/\varepsilon$ is the eddy viscosity. These forms are assumed to be valid approximations at high Reynolds numbers. For low Reynolds number or near-wall turbulence, viscous terms, as well as other near wall corrections, must be added to the RHS of Eqs. (55) and (56).

Second-order closures are based on the full Reynolds stress transport Eq. (25) as stated earlier. Models are needed for the pressure–strain correlation, the dissipation rate tensor, and the turbulent transport term. The former two terms are modeled as already discussed except the dissipation rate transport model has an anisotropic diffusion term where ν_T/σ_ε is replaced by the expression $C_\varepsilon(K/\varepsilon)\tau_{ij}$ in Eq. (56), where C_ε is a constant. Hence, for closure, we then only need an additional model for the third-order turbulent diffusion correlation

$$C_{ijk} \equiv \overline{u_i'u_j'u_k'} + \overline{p'u_i'}\delta_{jk} + \overline{p'u_j'}\delta_{ik}.$$

Typically, the pressure–diffusion correlation $\overline{p'u_i'}$ has been neglected, an assumption recently supported by DNS databases for turbulent channel flow. Then, $C_{ijk} \approx \overline{u_i'u_j'u_k'}$ is modeled alone. A gradient transport hypothesis of the general form

$$C_{ijk} = -\mathcal{D}_{ijk\ell mn}\frac{\partial \tau_{\ell m}}{\partial x_n} \tag{57}$$

is implemented. Some examples of previously proposed turbulent diffusion models of the form (57) are as follows.

Daly and Harlow[30] model:

$$C_{ijk} = -C_s\frac{K}{\varepsilon}\tau_{km}\frac{\partial \tau_{ij}}{\partial x_m} \tag{58}$$

Hanjalic and Launder[31] model:

$$C_{ijk} = -C_s\frac{K}{\varepsilon}\left(\tau_{im}\frac{\partial \tau_{jk}}{\partial x_m} + \tau_{jm}\frac{\partial \tau_{ik}}{\partial x_m} + \tau_{km}\frac{\partial \tau_{ij}}{\partial x_m}\right) \tag{59}$$

Mellor and Herring[32] model:

$$C_{ijk} = -\frac{2}{3}C_s\frac{K^2}{\varepsilon}\left(\frac{\partial \tau_{jk}}{\partial x_i} + \frac{\partial \tau_{ik}}{\partial x_j} + \frac{\partial \tau_{ij}}{\partial x_k}\right) \tag{60}$$

C_s is a constant that is usually taken to be approximately equal to 0.22 in the first model and 0.11 in the latter two models. Here, note that the Daly and Harlow[30] model does not satisfy the symmetry properties of the triple velocity correlation, unlike the other two models. The Hanjalic and Launder[31] model was obtained from a simplified analysis of the transport equation for the triple velocity correlation $\overline{u_i'u_j'u_k'}$; the Mellor and Herring[32] model follows from a partial isotropization of their expression. It should be noted that the Mellor and Herring[32] model has most often been used with a modeled transport equation for the turbulent length scale ℓ. Then, K^2/ε in Eq. (60) is replaced with $K^{1/2}\ell$; pressure–diffusion effects have usually then been additionally incorporated through the inclusion of a gradient transport model of the form

$$\overline{p'u_i'} \propto K^{\frac{1}{2}}\ell\frac{\partial K}{\partial x_i} \tag{61}$$

The Hanjalic and Launder[31] diffusion model has been used with the Launder et al.[33] model, whereas the Daly and Harlow[30] diffusion model has been used with the isotropization of production (IP) model, namely, the simplified form of the Launder et al.[33] model.[34] The Mellor and Herring[32] diffusion model has been implemented with the extended Rotta[35] pressure–strain model by Mellor and coworkers. (The resulting second-order closure has been termed the

Rotta–Kolmogorov model.) When these turbulent diffusion models are used in a full second-order closure, countergradient transport effects can be accounted for in a more systematic fashion.

The Launder et al.[33] model has been one of the most popular second-order closures. It is based on a linear pressure–strain model of the form (39) with $C_1 = 3.0$, $C_2 = 0.8$, $C_3 = 1.75$, and $C_4 = 1.31$. On the other hand, based on a dynamical systems approach, Speziale et al.[24] arrived at the variable coefficients $C_1 = 3.4 + 1.80\mathcal{P}/\varepsilon$, $C_2 = 0.8 - 1.30 II_b^{1/2}$, $C_3 = 1.25$, and $C_4 = 0.40$ where $II_b = b_{ij}b_{ij}$. (Here, we have neglected the quadratic return term, which is typically small in strained turbulent flows.) In equilibrium, this collapses to the constant form provided earlier. The Ref. 24 model has been demonstrated to perform somewhat better for a range of benchmark turbulent flows. It has the advantage that it can be integrated in wall-bounded geometries without the need for ad hoc wall reflection terms that can compromise the ability to apply a model in complex geometries, particularly in those containing corners.[36]

For turbulent flows that are not far from equilibrium, properly calibrated two-equation models can be used. Second-order closures are needed for turbulent flows that are far from equilibrium. However, the current generation of second-order closures does not do well when there are significant departures from equilibrium. In the next section, a new methodology is presented that alleviates this deficiency, and provides a bridge between second-order closures and two-equation models, thus yielding models that are more suitable for both time-dependent RANS and VLES.

IV. Combined Time-Dependent RANS and VLES Approach

Nonequilibrium extensions of the two-equation models and second-order closures discussed in Sec. III are now considered. It is essential for time-dependent RANS that Reynolds stress models be developed that are suitable for nonequilibrium turbulent flows. We can rewrite Eq. (50) in the form

$$\tau_{ij} = \tfrac{2}{3}K\delta_{ij} - \alpha_1^*(K^2/\varepsilon)\bar{S}_{ij} - \alpha_2^*(K^3/\varepsilon^2)(\bar{S}_{ik}\bar{\omega}_{kj} + \bar{S}_{jk}\bar{\omega}_{ki}) + \alpha_3^*(K^3/\varepsilon^2)\left(\bar{S}_{ik}\bar{S}_{kj} - \tfrac{1}{3}\bar{S}_{kl}\bar{S}_{kl}\delta_{ij}\right) \tag{62}$$

where

$$\alpha_i^* = \alpha_i\left(\frac{3}{3 - 2\eta^2 + 6\xi^2}\right) \tag{63}$$

for $i = 1, 2, 3$. Here, it can be shown that

$$\alpha_1 = \left(\tfrac{4}{3} - C_2\right)g, \qquad \alpha_2 = \tfrac{1}{2}\left(\tfrac{4}{3} - C_2\right)(2 - C_4)g^2$$

$$\alpha_3 = \left(\tfrac{4}{3} - C_2\right)(2 - C_3)g^2, \qquad g = \left(\tfrac{1}{2}C_1 + (\mathcal{P}/\varepsilon) - 1\right)^{-1} \tag{64}$$

$$\eta = \tfrac{1}{2}(\alpha_3/\alpha_1)(K/\varepsilon)(\bar{S}_{ij}\bar{S}_{ij})^{\frac{1}{2}}, \qquad \xi = (\alpha_2/\alpha_1)(K/\varepsilon)(\bar{\omega}_{ij}\bar{\omega}_{ij})^{\frac{1}{2}}$$

with the constants $C_1 - C_4$ as given before and $\mathcal{P}/\varepsilon$ given by Eq. (44) (Ref. 26).

Use will now be made of the RDT solution for homogeneous shear flow. In this solution we consider an initially isotropic turbulence subjected to a uniform shear, with shear rate S, where $SK_0/\varepsilon_0 \gg 1$ given that K_0 and ε_0 are the initial turbulent kinetic energy and dissipation rate. (The mean velocity gradient tensor in this case is given by $\partial\bar{u}_i/\partial x_j \equiv S\delta_{1i}\delta_{2j}$.) This constitutes a far from equilibrium test case because it is known that, in homogeneous shear flow, an equilibrium value of $SK/\varepsilon \approx 5$ is ultimately achieved.[37] The RDT solution, which is obtained from solving the linearized Navier–Stokes equations, is formally an excellent approximation to the full nonlinear Navier–Stokes equations for short elapsed times under a rapid distortion, i.e, for a fraction of an eddy turnover time where $\varepsilon_0 t/K_0 < 1$. The long time asymptotic RDT solution (in the limit as $t^* \to \infty$, where $t^* = St$) has been recently obtained analytically by Rogers,[38] who corrected some previously published errors. This asymptotic RDT solution is given by

$$\tau_{12}/K_0 = -2\,\ell n 2 \tag{65}$$

$$K^* = (2\,\ell n 2)t^* \tag{66}$$

$$b_{11} = \tfrac{2}{3}, \qquad b_{22} = b_{33} = -\tfrac{1}{3} \tag{67}$$

where $K^* \equiv K/K_0$. In obtaining this solution, use has been made of

$$\dot{K}^* = -(\tau_{12}/K_0) \tag{68}$$

in the RDT limit of homogeneous shear flow. This asymptotic solution is approached fairly fast, i.e., by the time $St \approx 10$. For sufficiently large shear rates $SK_0/\varepsilon_0 \gg 1$ (which are required for the RDT approximation), we are guaranteed that the required constraint of $\varepsilon_0 t/K_0 < 1$ is still satisfied at that time.

The key elements of the RDT solution for homogeneous shear flow just given are as follows: 1) the turbulent kinetic energy K^* grows linearly so that $\dot{K}^*$ remains bounded and of order one, and 2) the normal Reynolds stress anisotropies approach a one-component state where $b_{11} = \frac{2}{3}$, $b_{22} = -\frac{1}{3}$, and $b_{33} = -\frac{1}{3}$ (and, hence, all of the energy is concentrated in the streamwise component). DNS results of Lee et al.[39] indicate that this happens in a fraction of an eddy turnover time.

From Eq. (62), it is clear that

$$(\tau_{12}/K_0) = -\tfrac{1}{2}\alpha_1^*(SK/\varepsilon)(K/K_0) \tag{69}$$

in homogeneous shear flow. Because, in the RDT solution, $SK/\varepsilon \to \infty$ whereas K/K_0 remains of order one, it is obvious from Eqs. (62–66) that

$$\alpha_1^* \sim 1/\eta \tag{70}$$

where we have made use of the fact that $\eta \propto \xi \propto SK/\varepsilon$ in homogeneous shear flow. It is clear that the equilibrium model, encompassed by Eq. (63), violates this constraint. This problem can be remedied via a Padé approximation whereby Eq. (63) is replaced by a regularized expression that is approximately equal to Eq. (63) for the near-equilibrium case (where $\eta < 1$) but has the correct asymptotic behavior, given in Eq. (70), for $\eta \gg 1$. One such approximation, which is accurate to $\mathcal{O}(\eta^4)$, is as follows[27]:

$$\alpha_1^* = \frac{(1 + 2\xi^2)(1 + 6\eta^5) + \frac{5}{3}\eta^2}{(1 + 2\xi^2)\left(1 + 2\xi^2 + \eta^2 + 6\beta_1\eta^6\right)}\alpha_1 \tag{71}$$

where β_1 is an arbitrary constant. Equation (71) is regular for all values of η and ξ, thus removing the singularity in Eq. (63). It yields results that are within 1% of Eq. (63) for near-equilibrium turbulent flows (where the latter is valid) and has the correct asymptotic behavior of $\alpha_1^* \sim 1/\eta$ for $\eta \gg 1$. Equations (65) and (66) suggest that β_1 is in the range of 5–10. The value of $\beta_1 \approx 7$ has been arrived at.[27]

Whereas the regularized expression (51), derived by Gatski and Speziale,[26] is asymptotically consistent for the b_{11}, b_{22}, and b_{33} components, it does not yield the correct tendency to a one-component state in the RDT limit. This can be remedied by the alternative regularized form, obtained by a Padé approximation that is accurate to $\mathcal{O}(\eta^4)$ (Ref. 27)

$$\alpha_i^* = \frac{(1 + 2\xi^2)(1 + \eta^4) + \frac{2}{3}\eta^2}{(1 + 2\xi^2)\left(1 + 2\xi^2 + \beta_i\eta^6\right)}\alpha_i \tag{72}$$

where β_i is an arbitrary constant ($i = 2, 3$). Equation (72) represents an excellent approximation to Eq. (63) for near-equilibrium turbulent flows, where $\eta < 1$. It is regular for all values of η and ξ, has the correct asymptotic behavior for $\eta \gg 1$, and, for values of β_2 and β_3 of approximately 5, predicts an approach to a one component state consistent with RDT of homogeneous shear flow. The specific values of $\beta_2 \approx 6$ and $\beta_3 \approx 4$ have been arrived at by Speziale and Xu.[27] The idea here is to develop a model that will perform well for a wide range of shear rates because shear flows form such a cornerstone of engineering calculations. This will be discussed in more detail in Sec. V.

Second-order closures that are suitable for nonequilibrium turbulent flows can then be obtained by conducting a relaxation time approximation around the nonequilibrium extension of the explicit

algebraic stress model (ASM) given by Eqs. (62), (71), and (72). The idea of obtaining second-order closures by a relaxation time approximation around an equilibrium algebraic model is probably first attributable to Saffman.[40] (This stood in contrast with the more commonly adopted approach of directly modeling the higher-order correlations that appear in the Reynolds stress transport equation, which was popular even before Launder et al.[33]) However, Saffman[40] implemented this relaxation time approximation around a simple, nonlinear algebraic representation for the Reynolds stress tensor. In contrast to that approach, we have implemented a relaxation time approximation about the nonequilibrium extension of the explicit ASM written in terms of the Reynolds stress anisotropy tensor. (In strained homogeneous turbulent flows, it is only the Reynolds stress anisotropy tensor that equilibrates; the Reynolds stresses grow exponentially.) Hence, we have proposed the relaxation model

$$\dot{b}_{ij} = -C_R(\varepsilon/K)\left(b_{ij} - b_{ij}^{E^*}\right) \tag{73}$$

where

$$b_{ij}^{E^*} = -\tfrac{1}{2}\alpha_1^*(K/\varepsilon)\bar{S}_{ij} - \tfrac{1}{2}\alpha_2^*(K^2/\varepsilon^2)(\bar{S}_{ik}\bar{\omega}_{kj} + \bar{S}_{jk}\bar{\omega}_{ki}) + \tfrac{1}{2}\alpha_3^*(K^2/\varepsilon^2)\left(\bar{S}_{ik}\bar{S}_{kj} - \tfrac{1}{3}\bar{S}_{kl}\bar{S}_{kl}\delta_{ij}\right)$$

is the nonequilibrium extension of Eq. (62), written in terms of the Reynolds stress anisotropy tensor, with α_1^*–α_3^* given by their nonequilibrium forms (71) and (72). In Eq. (73), C_R is a dimensionless relaxation coefficient. Consistency with the Crow constraint (which is important, to capture the early time behavior) requires that

$$C_R = \frac{8}{15}\left(\frac{3-2\eta^2}{3\alpha_1}\right) \tag{74}$$

in an initially isotropic turbulence subjected to a mild strain. Of course, for strongly strained turbulent flows, Eq. (74) must be regularized. One preliminary form that has been considered, motivated by Eq. (71), is given by[27]

$$C_R = \frac{8}{15\alpha_1}\frac{1+\eta^2+6\beta_1\eta^6}{1+\frac{5}{3}\eta^2+6\eta^5} \tag{75}$$

When Eq. (73) is rearranged into a transport equation for the Reynolds stress tensor, it yields a model that differs from the traditional models in a notable way: the rapid pressure–strain correlation depends linearly on the Reynolds stress anisotropy tensor, but depends nonlinearly on the invariants of the rotational and irrotational strain rates to the lowest order, i.e.,

$$\mathcal{M}_{ijkl} = \mathcal{M}_{ijkl}(\boldsymbol{b};\eta,\xi) \tag{76}$$

This is consistent with the rapid pressure–strain correlation, which by definition is linear in the energy spectrum tensor and, hence, linear in the Reynolds stress tensor.[29] Models for the rapid pressure–strain correlation that are fully nonlinear in b_{ij} are fundamentally inconsistent. In the next section, we will see that this new approach leads to a notable improvement in the description of homogeneous shear flow under a wide range of shear rates.

For inhomogeneous turbulent flows, the time derivative on the left-hand side of Eq. (73) is replaced with the mean convective derivative, and turbulent diffusion terms are added. This yields the form

$$\frac{\mathrm{D}b_{ij}}{\mathrm{D}t} = -C_R\frac{\varepsilon}{K}\left(b_{ij} - b_{ij}^{E^*}\right) + \frac{\partial}{\partial x_k}\left(\frac{\nu_T}{\sigma_b}\frac{\partial b_{ij}}{\partial x_k}\right) \tag{77}$$

where $\nu_T \equiv C_\mu K^2/\varepsilon$ is the eddy viscosity and σ_b is a constant. This methodology allows for the development of computer codes, where a two-equation model can be automatically upgraded to a full second-order closure as needed. In addition, this two-equation model has builtin nonequilibrium extensions that, in some ways, allows it to outperform existing second-order closures. This will be discussed in more detail in the next section.

In the approach to subgrid-scale modeling that the author is considering, great care is taken to ensure the following.

1) Any test filters or double-filtered fields must be absent from the subgrid-scale models that can significantly contaminate the large scales and necessitate the inversion of filtered quantities that must be avoided. (This is equivalent to solving a Fredholm integral equation of the first kind, which is ill-posed in a mathematical sense.)

2) A systematically derived anisotropic eddy viscosity must be incorporated that is strain dependent and allows for the direct integration of subgrid-scale models to a solid boundary without the need for any ad hoc wall damping functions.[41]

3) A state-of-the-art Reynolds stress model must be recovered in the coarse mesh/infinite Reynolds number limit so that an LES goes continuously to a RANS computation.

In mathematical terms, this can be accomplished by models of the form

$$\tau_{ij} = [1 - \exp(-\beta\Delta/L_K)]^n \tau_{ij}^{(R)} \tag{78}$$

for the subgrid-scale stress tensor τ_{ij}, where $\tau_{ij}^{(R)}$ is a Reynolds stress model, Δ is the computational mesh size, L_K is the Kolmogorov length scale, and β and n are constants. In the limit as $\Delta/L_K \to 0$, all relevant scales are resolved, and we have a direct simulation where $\tau_{ij} = 0$; as $\Delta/L_K \to \infty$ and the mesh becomes coarse or the Reynolds number becomes extremely large, we recover a Reynolds stress model and an RANS computation. In between these two limits, we have an LES or a VLES (the latter denotes an LES where the preponderance of the turbulent kinetic energy is unresolved; also see Ref. 42). Here, note that, in the simulation of turbulence, the mesh is fine (or coarse) depending on whether Δ is small (or large) compared to the Kolmogorov length scale $L_K \equiv \nu^{3/4}/\varepsilon^{1/4}$. This automatically brings in a dependence on the turbulence Reynolds number ($Re_t \equiv K^2/\nu\varepsilon$) because $L_K = Re_t^{-3/4}K^{3/2}/\varepsilon$. An estimate of the Kolmogorov length scale is provided by the modeled transport equation for ε, discussed earlier, in Eq. (56). To estimate the Kolmogorov length scale to within 10%, it is only required that the dissipation rate be estimated to within 50%. Hence, it is quite reasonable to expect that an acceptable estimate of the Kolmogorov length scale can be obtained (this is a crucial element of this proposed approach). The Reynolds stress model in Eq. (78) can be represented by the forms discussed in this section. A two-equation model, which is upgraded to a second-order closure as needed via the relaxation time approximation, is recommended for $\tau_{ij}^{(R)}$. It was recently shown by Speziale and Abid[41] that these two-equation models can be integrated directly to a solid boundary with no wall damping functions; only the singularity in the ε-transport equation needs to be removed.

Some comments are needed concerning the choice of a filter in this new approach to LES and the melding together of spatial filtering in LES and Reynolds averaging in RANS. We want a filter that yields the minimum contamination of the large scales. The reason for this is clear; defiltering must be avoided because it constitutes an ill-posed mathematical problem as stated earlier. The purpose of practical LES is to predict the Reynolds-averaged fields. To do so, the filtered velocity, which is calculated, must invariably be used to estimate the large-scale part of the instantaneous velocity, which then yields the Reynolds-averaged fields through appropriate ensemble averages. The filtered equations of motion (10) are of the same form as the Reynolds-averaged equations (23). It is envisoned that ensemble averages will also be taken even if we are conducting a time-dependent RANS. Thus, we do not need to know the effect of the filter, which can never be fully known in complex geometries, except perhaps for model calibration in benchmark flows. This allows us to meld together the LES and RANS methodology, which are normally treated as disparate approaches.

In both of these approaches we calculate what is tantamount to the large-scale velocity field, through the same basic equations of motion, and then obtain the Reynolds-averaged fields through ensemble averages. The large scales make the dominant contribution to the most pertinent fields such as the turbulent kinetic energy. A minimum contamination of the large scales can be accomplished with, of the order of, a 128^3 computational mesh using a filter with a compact support, such as the box filter, which has a small filter width of, for example, two mesh points. Some of the previously conducted coarse grid LES (which has typically had no more than 32^3 mesh points) must be avoided wherein the filter width at times has

been as much as 25% of the computational domain, significantly contaminating the large scales. Besides, recent increases in computational capacity have begun to make 128^3 computations much more feasible for engineering calculations. (A small compromise to 100^3 computations can always be made.) In addition, it should be noted that practical LES, in complex geometries, will require the use of finite difference techniques with a compact filter, where we will never make explicit use of the filter. (These finite difference methods should be based on fourth-order accurate finite difference schemes.) Some illustrative calculations will be provided in the next section to demonstrate the potential of this new approach for practical engineering calculations.

V. Illustrative Calculations

First, the performance of this approach to Reynolds stress modeling in benchmark turbulent flows, near equilibrium, will be demonstrated by several examples. The two-equation model discussed herein will be predominantly considered because two-equation models are recommended for engineering calculations at this time. One of the nontrivial test cases that has been considered in recent years is homogeneous shear flow in a rotating frame. Here, a system rotation can either stabilize or destabilize the turbulence in shear flow. In this flow, an initially isotropic turbulence (with turbulent kinetic energy K_0 and turbulent dissipation rate ε_0) is suddenly subjected to a uniform shear with constant shear rate S in a reference frame rotating steadily with angular velocity Ω. The mean velocity gradient tensor and the angular velocity vector of the reference frame are given by

$$\frac{\partial \bar{u}_i}{\partial x_j} = S\delta_{1i}\delta_{2j}, \qquad \Omega_i = e_{i12}\Omega \tag{79}$$

In Figs. 1a–1c, the time evolution of the turbulent kinetic energy predicted by this new two-equation model is compared with the LES of Bardina et al.,[11] as well as with the predictions of the standard K–ε model and the full Ref. 24 second-order closure on which it is based. From these results, it is clear that the new two-equation model yields the correct growth rate for pure shear flow ($\Omega/S = 0$) and properly responds to the stabilizing effect of the rotations $\Omega/S = 0.5$ and -0.5. These results are remarkably close to those obtained from the full Ref. 24 second-order closure, as shown in Fig. 1. In contrast to these results, the standard K–ε model overpredicts the growth rate of the turbulent kinetic energy in pure shear flow ($\Omega/S = 0$) and fails to predict the stabilizing effect of the rotations shown in Figs. 1b and 1c. Because the standard K–ε model makes use of the Boussinesq eddy viscosity hypothesis, it is oblivious to the application of a system rotation, i.e., it yields the same solution for all values of Ω/S. The new two-equation model predicts unstable flow only for the intermediate band of rotation rates $-0.09 \le \Omega/S \le 0.53$; this is generally consistent with linear stability theory that predicts unstable flow for $0 \le \Omega/S \le 0.5$ (Ref. 43). In contrast to these results, the Launder et al.[33] model and the IP model prematurely restabilize at $\Omega/S \approx 0.37$.

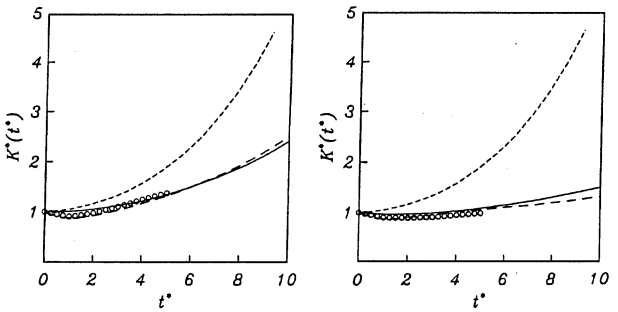

a) $\Omega/S = 0$ b) $\Omega/S = 0.5$

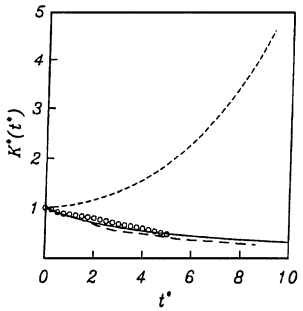

c) $\Omega/S = -0.5$ (from Ref. 26)

Fig. 1 Time evolution of the turbulent kinetic energy in rotating homogeneous shear flow; comparison of the model predictions with the large-eddy simulations of Bardina et al.[11]: ——, new explicit ASM; – – –, SSG model; - - - -, K–ε model; and ○, LES.

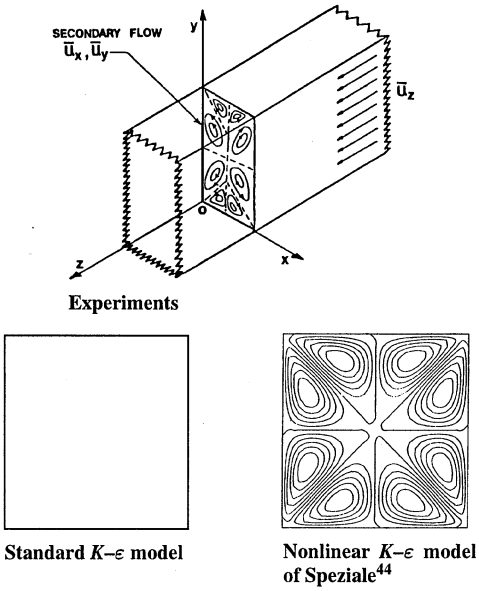

Fig. 2 Turbulent secondary flow in a rectangular duct.

Two examples will now be presented that illustrate the enhanced predictions that are obtained for turbulent flows exhibiting effects arising from normal Reynolds stress differences. Here, we will show results obtained from the nonlinear K–ε model of Speziale[44] (also see Refs. 45 and 46). For turbulent shear flows that are predominantly unidirectional, with secondary flows or recirculation zones driven by small normal Reynolds stress differences, a quadratic approximation to the anisotropic eddy viscosity model discussed herein collapses to the nonlinear K–ε model.[26] In Fig. 2, it is demonstrated that the nonlinear K–ε model predicts an eight-vortex secondary flow, in a square duct, in line with experimental observations; on the other hand, the standard K–ε model erroneously predicts that there is no secondary flow. To be able to predict secondary flows in noncircular ducts, the axial mean velocity $\bar{u}_z$ must give rise to a nonzero normal Reynolds stress difference $\tau_{yy} - \tau_{xx}$. This requires an anisotropic eddy viscosity. (Any isotropic eddy viscosity, including that used in the standard K–ε model, yields a vanishing normal Reynolds stress difference, which makes it impossible to describe these secondary flows.)

In Fig. 3, results obtained from the nonlinear K–ε model are compared with the experimental data of Kim et al.[47] and Eaton and Johnston[48] for turbulent flow past a backward facing step. It is clear that these results are excellent: Reattachment is predicted at $x/H \approx 7.0$ in close agreement with the experimental data (Fig. 3a). The Reynolds shear stresses are also well represented by the model (Fig. 3b). In contrast to these results, the standard K–ε model predicts reattachment at $x/H \approx 6.25$, an 11% underprediction. This error predominantly results from the inaccurate prediction of normal Reynolds stress anisotropies in the recirculation zone as discussed by Speziale and Ngo.[49]

As has been alluded to, the new two-equation model can be integrated directly to a solid boundary with no wall damping. In Fig. 4, the skin-friction coefficient obtained from this model, plotted as function of the Reynolds number based on the momentum thickness, Re_θ, is compared with experimental data[50] and with results obtained from the K–ε model with wall damping.[51] Clearly, the results are

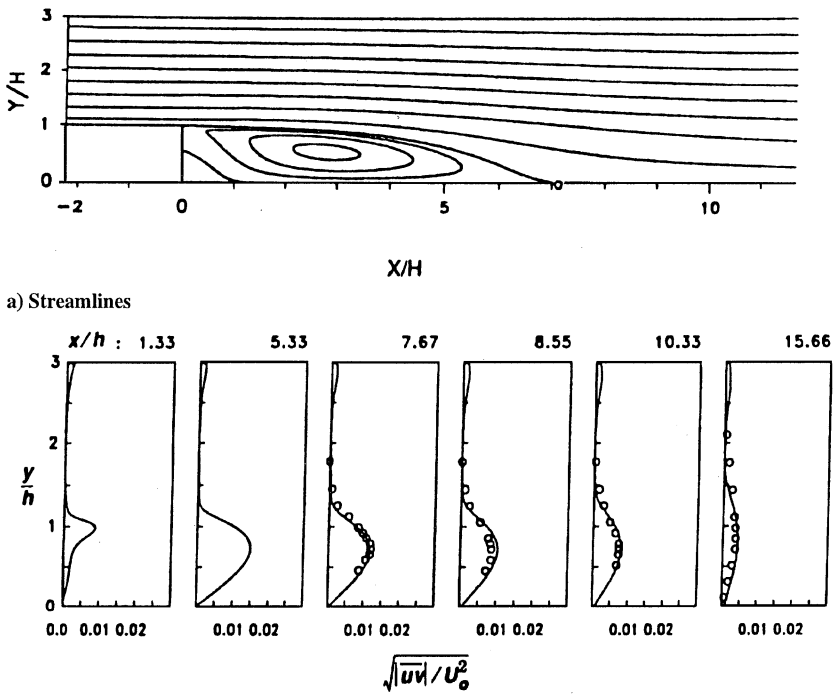

a) Streamlines

b) Turbulent shear stress profiles

Fig. 3 Turbulent flow past a backward facing step; comparison of the predictions of the nonlinear K–ε model with experiments: ——, computations with anisotropic eddy viscosity and ○, experimental mean reattachment point (experiments of Kim et al.[47]; Eaton and Johnston[48]).

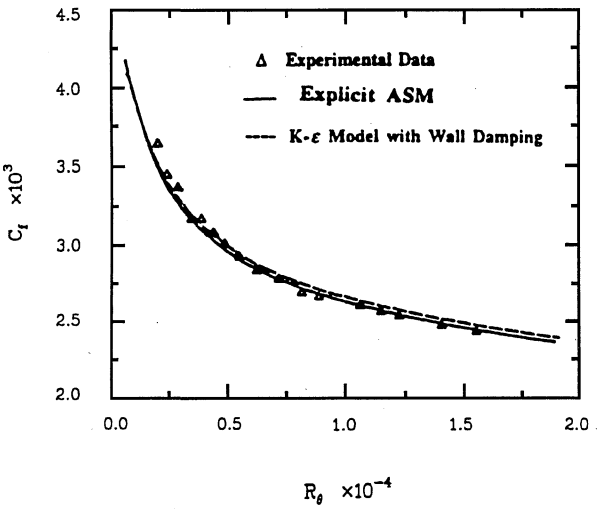

Fig. 4 Comparison of the predictions of the explicit ASM of Gatski and Speziale[26] for skin friction with experimental data[50] for the flat plate turbulent boundary layer.

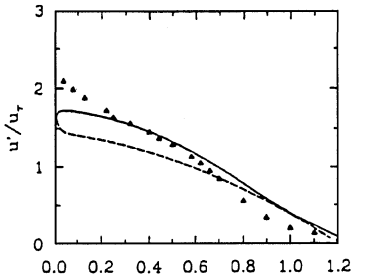

Streamwise turbulence intensity

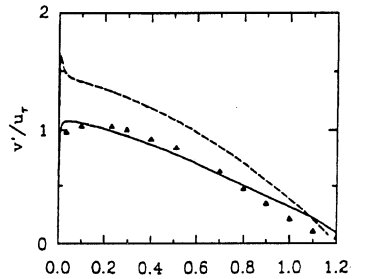

Turbulence intensity normal to wall

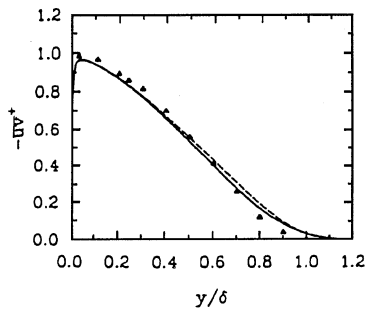

Turbulent shear stress

Fig. 5 Turbulent flat plate boundary layer; comparison of the predictions of the new two-equation model (——) and the Speziale et al.[51] model (- - -) with experimental data (△).[50]

extremely good. No wall damping functions are needed; the singularity, which occurs at the wall, only needs to be removed from the dissipation rate equation.[42] Excellent predictions for the Reynolds stresses are obtained starting in the log-layer shown in Fig. 5, where the turbulence intensities are given. A Reynolds stress model cannot be expected to accurately describe the turbulence structure immediately adjacent to a wall because it exhibits such a wide range of scales and diverse turbulence physics. We only need to have Reynolds stress models that can operationally be integrated to a wall without compromising their predictive capabilities away from the wall.

The two-equation model discussed has recently been shown to be feasible for complex aerodynamic computations by Abid et al.[28] using the alternative regularization procedure discussed earlier. The ONERA M6 wing at a Mach number of $M_\infty = 0.8447$ with an angle of attack of $\alpha = 5.06$ deg and a Reynolds number of $Re = 11.7 \times 10^6$ has been considered.[52] At this Mach number the turbulence behaves as if it were incompressible. (Compressibility effects are

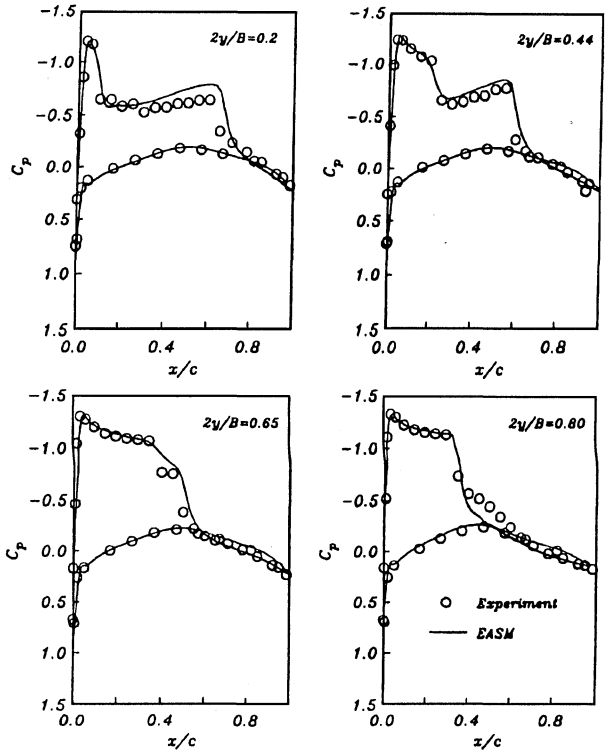

Fig. 6 Surface pressure distributions for the ONERA M6 wing at four different spanwise locations.

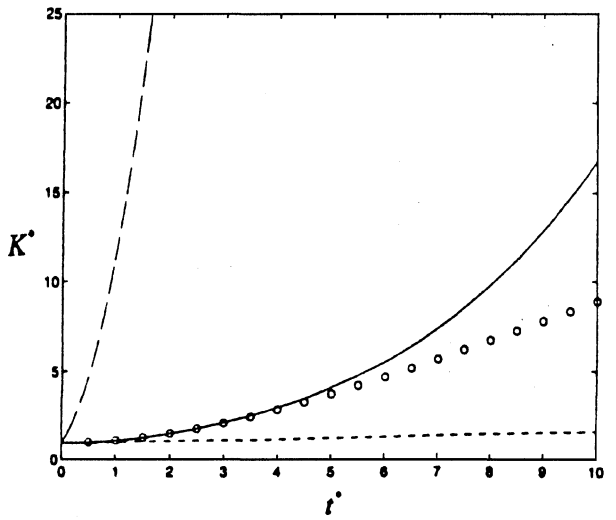

Fig. 7 Time evolution of the turbulent kinetic energy in homogeneous shear flow; comparison of the model predictions for the far from equilibrium initial condition $SK_0/\varepsilon_0 = 50$ with RDT: ——, Ref. 24 model; – – –, K–ε model; - - - -, explicit ASM of Gatski and Speziale[26]; and ○, RDT.

only felt through changes in the mean density because the Morkovin hypothesis applies.) In Fig. 6, a comparison is made of the computed surface pressure distributions with experiments[52] at four different spanwise locations. As can be seen, the results are quite good.

Now, we will consider the far from equilibrium test case in homogeneous shear flow where $SK_0/\varepsilon_0 = 50$; for this strongly sheared case, RDT constitutes a good approximation for early times. In Fig. 7, the time evolution of the turbulent kinetic energy predicted by several models is compared with the RDT solution.[38] It is clear from these results that none of the models are able to predict the correct trend. (DNS results have tended to indicate that, for this case, RDT is a good approximation until $St \approx 12$.) The interesting point here is that the Ref. 24 second-order closure predicts too large a growth rate whereas the explicit ASM of Gatski and Speziale,[26] based on the Ref. 24 model, yields a growth rate that is far too low. Here, the former problem arises because pressure–strain models of the form (38) do not apply to turbulent flows that are far from equilibrium; the latter problem is because the regularization procedure used by Gatski and Speziale[26] does not apply to turbulent flows that are strongly strained. (The eddy viscosity $\nu_T \sim 1/\eta^2$ instead of as $1/\eta$, which explains the low growth rate in this case.) On the other hand, the standard K–ε model renders $\nu_T \sim \mathcal{O}(1)$, which explains its enormous growth rate. (The standard K–ε model erroneously predicts that $K^* \to \infty$ as $\eta \to \infty$.)

Next, results will be presented for the nonequilibrium extension of the two-equation model discussed in Sec. 4. The results correspond to the choice of constants

$$\beta_1 = 7.0, \qquad \beta_2 = 6.3, \qquad \beta_3 = 4.0 \tag{80}$$

in the regularized coefficients α_1^*–α_3^* given in Eqs. (71) and (72). The predictions of the new explicit ASM for the time evolution of the turbulent kinetic energy are compared in Fig. 8 with the RDT solution for the same far from equilibrium test case in homogeneous shear flow, where $SK_0/\varepsilon_0 = 50$. With this new nonequilibrium extension, the results are remarkably improved. It is not even necessary to introduce the relaxation time approximation. [From Eq. (75), the relaxation coefficient is large for this case, rendering its effect small on K^*.] In Fig. 9, the time evolution of the normal components of the Reynolds stress anisotropy tensor obtained from the new relaxation

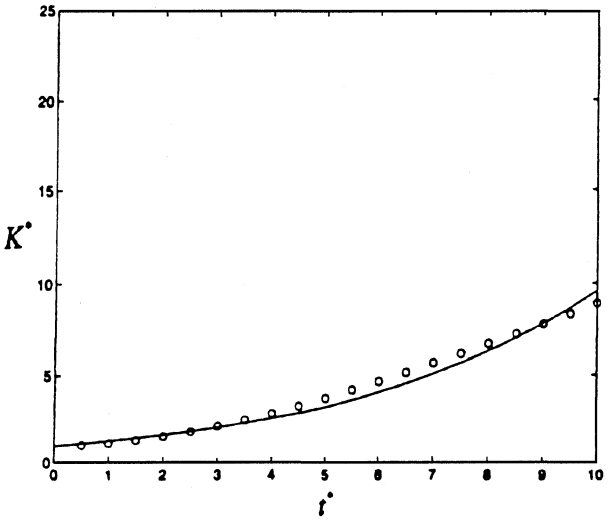

Fig. 8 Comparison of the predictions of the new nonequilibrium extension of the explicit ASM for $SK_0/\varepsilon_0 = 50$ (——) with RDT for the time evolution of the turbulent kinetic energy in homogeneous shear flow (○).

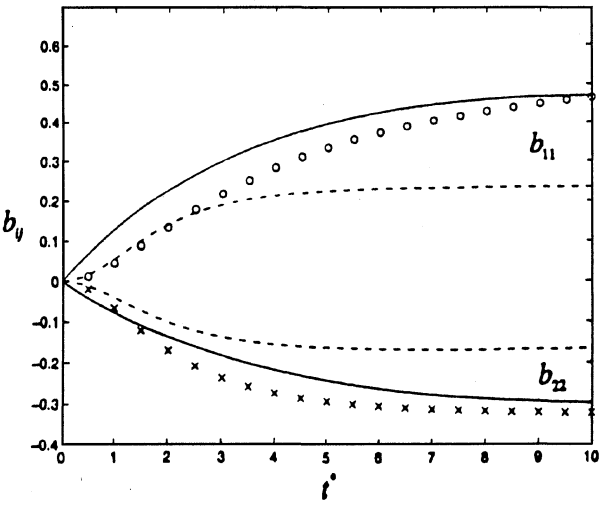

Fig. 9 Time evolution of the Reynolds stress anisotropies in homogeneous shear flow; comparison of the model predictions for $SK_0/\varepsilon_0 = 50$ with RDT: – – –, Ref. 24 model; ——, new relaxation model; and ○, ×, RDT.

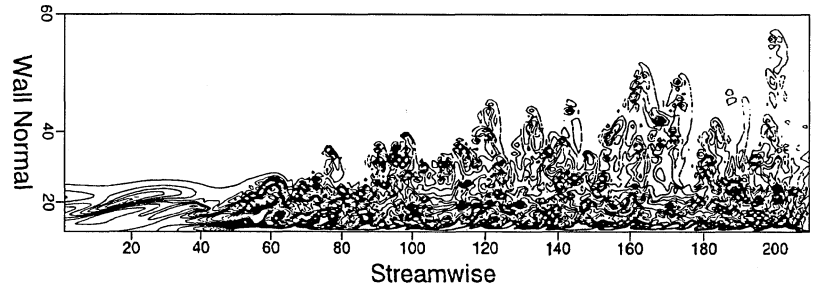

Fig. 10 Plot of spanwise vorticity in the developing turbulent boundary layer obtained from LES (computations done by Fasel and co-workers at the University of Arizona).

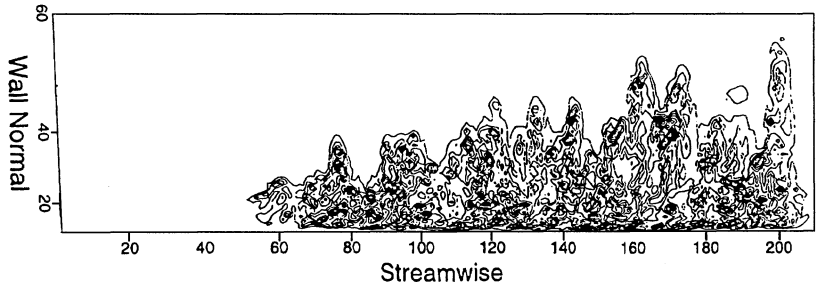

Fig. 11 Plot of the eddy viscosity in the developing turbulent boundary layer obtained from LES (computations done by Fasel and co-workers at the University of Arizona).

model (73) (for $SK_0/\varepsilon_0 = 50$) is compared with RDT, as well as with the predictions of the Ref. 24 second-order closure. Here again, the new model yields a substantial improvement, rendering results that are more properly in line with an approach to a one-component state. Note these results are somewhat preliminary because the relaxation coefficient C_R has not been completely finalized. (There are ambiguities that remain in what regularization procedure is implemented.) These questions are currently being investigated and should be resolved soon. The ability to predict shear flows over a wide range of shear rates should lead to an enhanced time-dependent RANS capability in engineering applications.

Finally, some preliminary LES results will be shown for the developing turbulent boundary layer, integrated through transition. These computations were conducted by Fasel and his group at the University of Arizona using an empirically based ramp function, which depends explicitly on the momentum thickness Reynolds number and the mesh size with a simple eddy viscosity model, as a preliminary test of the ideas embodied in Eq. (78). In Fig. 10, the spanwise vorticity obtained from the LES is shown, which compares favorably with the corresponding results obtained from DNS. It is clear that the subgrid-scale model allows the LES to pick up the pertinent flow structures and to be integrated through transition (laminar–turbulent flow). The ramp function, which forms a central part of Eq. (78), allows the eddy viscosity to gradually turn on as the flow becomes turbulent. In this regard, the corresponding eddy viscosity is displayed in Fig. 11. These preliminary results are extremely encouraging and demonstrate the potential of this new approach for LES and time-dependent RANS.

VI. Conclusions

There is a relatively sound theoretical basis for the existing type of Reynolds stress models in two-dimensional mean turbulent flows that are close to equilibrium and only weakly inhomogeneous. A new generation of two-equation models and second-order closures has emerged that provides a surprisingly good description of these flows in a variety of benchmark situations. Here, the former models are systematically derived from the latter in the equilibrium limit, thus providing a direct link between these two basic types of closures. Whereas the belief that Reynolds stress models are completely ad hoc is largely warranted for the older eddy viscosity models of turbulence, it constitutes a far too pessimistic assessment of the current generation of Reynolds stress closures. A range of benchmark turbulent flows, near equilibrium, are increasingly well described as demonstrated herein, and nonequilibrium effects are beginning to be built into these models making them more suitable for time-dependent RANS. This work has contributed greatly to establishing even a more definitive link between two-equation models and second-order closures through the relaxation time approximation discussed.

Some comments are in order concerning the role of direct simulations and LES in turbulence. There is no question that DNS, and the computer in general, has revolutionized the study of turbulence. DNS has already shed new light on the physics of a range of basic turbulent flows and the future potential is enormous. It already appears that in the not too distant future DNS will entirely replace basic benchmark physical experiments for homogeneous turbulence and near-wall turbulent flows, at lower turbulence Reynolds numbers. The same may also be true for basic compressible turbulent flows. However, it appears that DNS will, for a long time to come, be limited to relatively simple geometries and low to moderate turbulence Reynolds numbers. Direct simulations of the kind of complex turbulent flows of technological importance, at high turbulence Reynolds numbers, discussed earlier could require the generation of databases with upwards of 10^{20} numbers. Even if such computer capacity became available in the foreseeable future, and that is extremely doubtful, it is questionable as to whether this would constitute a truly satisfactory solution. For example, would one consider as satisfactory a solution to laminar channel flow that consisted of the tracking of 10^{23} molecules? The answer is: certainly not from an engineering standpoint. As far as LES is concerned, it must again be said that it has never lived up to its initial promise. Because practical LES at high-turbulence Reynolds numbers requires that a significant fraction of the turbulent kinetic energy be left unresolved, the same type of uncertainties exist with subgrid-scale models as with Reynolds stress models, particularly in wall-bounded flows. The way that traditional LES has been formulated is probably only suitable for doing less expensive parametric studies of benchmark direct simulations once the reliability of the subgrid-scale model has been established by DNS for the baseline case. Three-dimensional, time-dependent RANS or VLES, based on a state-of-the-art Reynolds stress model, will probably be applied to complex turbulent flows in the future in some form. This alternative approach to LES discussed herein can serve as a bridge between DNS, LES, and RANS. The results obtained already are highly encouraging and further tests are currently underway.

Acknowledgments

The author gratefully acknowledges the support provided by the Office of Naval Research under Grant N00014-94-1-0088 (Accelerated Research Initiative on Nonequilibrium Turbulence, L. P. Purtell, Program Officer). Private communications from W. C. Reynolds (1985), M. M. Rogers (1995), and H. Fasel (1996) are also acknowledged.

References

[1]Smagorinsky, J., "General Circulation Experiments with the Primitive Equations," *Month. Weath. Rev.*, Vol. 93, 1963, pp. 99–165.

[2]Deardorff, J. W., "A Numerical Study of Three-Dimensional Turbulent Channel Flow at Large Reynolds Numbers," *Journal of Fluid Mechanics*, Vol. 41, 1970, pp. 453–480.

[3]Leonard, A., "On the Energy Cascade in Large-Eddy Simulations of Turbulent Flows," *Advances in Geophysics A*, Vol. 18, 1974, pp. 237–248.

[4]Ferziger, J. H., "Large-Eddy Simulation of Turbulent Flows," AIAA Paper 76-347, Jan. 1976.

[5]Clark, R. A., Ferziger, J. H., and Reynolds, W. C., "Evaluation of Subgrid-Scale Models Using an Accurately Simulated Turbulent Flow," *Journal of Fluid Mechanics*, Vol. 91, 1976, pp. 1–16.

[6]Erlebacher, G., Hussaini, M. Y., Speziale, C. G., and Zang, T. A., "Toward the Large-Eddy Simulation of Compressible Turbulent Flows," *Journal of Fluid Mechanics*, Vol. 238, 1992, pp. 155–185.

[7]Rogallo, R. S., and Moin, P., "Numerical Simulation of Turbulent Flows," *Annual Review of Fluid Mechanics*, Vol. 16, 1984, pp. 99–137.

[8]Biringen, S., and Reynolds, W. C., "Large-Eddy Simulation of the Shear Free Turbulent Boundary Layer," *Journal of Fluid Mechanics*, Vol. 103, 1981, pp. 53–63.

[9]Moin, P., and Kim, J., "Numerical Investigation of Turbulent Channel Flow," *Journal of Fluid Mechanics*, Vol. 118, 1982, pp. 341–377.

[10]Speziale, C. G., "Galilean Invariance of Subgrid Scale Models in the Large-Eddy Simulation of Turbulence," *Journal of Fluid Mechanics*, Vol. 156, 1985, pp. 55–62.

[11]Bardina, J., Ferziger, J. H., and Reynolds, W. C., "Improved Turbulence Models Based on Large-Eddy Simulation of Homogeneous, Incompressible Turbulent Flows," Dept. of Mechanical Engineering, TR TF-19, Stanford Univ., Stanford, CA, May 1983.

[12]Piomelli, U., Ferziger, J. H., and Moin, P., "Models for Large-Eddy Simulations of Turbulent Channel Flows Including Transpiration," Dept. of Mechanical Engineering, TR TF-32, Stanford Univ., Stanford, CA, Dec. 1987.

[13]Schumann, U., "Subgrid Scale Models for Finite Difference Simulations of Turbulent Flows in Plane Channels and Annuli," *Journal of Computational Physics*, Vol. 18, 1975, pp. 376–404.

[14]Schumann, U., "Large-Eddy Simulation of the Upslope Boundary Layer," *Quarterly of the Journal of the Royal Meteorological Society*, Vol. 116, 1990, pp. 637–670.

[15]Speziale, C. G., Erlebacher, G., Zang, T. A., and Hussaini, M. Y., "The Subgrid Scale Modeling of Compressible Turbulence," *Physics of Fluids*, Vol. 31, 1988, pp. 940–942.

[16]Erlebacher, G., Hussaini, M. Y., Speziale, C. G., and Zang, T. A., "On the Large-Eddy Simulation of Compressible Isotropic Turbulence," *Lecture Notes in Physics*, Vol. 371, 1990, pp. 121–126.

[17]Germano, M., Piomelli, U., Moin, P., and Cabot, W. H., "A Dynamic Subgrid-Scale Eddy Viscosity Model," *Physics of Fluids A*, Vol. 3, 1991, pp. 1760–1765.

[18]Hussaini, M. Y., Speziale, C. G., and Zang, T. A., "Discussion of the Potential and Limitations of Direct and Large-Eddy Simulations," *Lecture Notes in Physics*, Vol. 357, 1990, pp. 354–368.

[19]Hinze, J. O., *Turbulence*, 2nd ed., McGraw–Hill, New York, 1975.

[20]Launder, B. E., and Spalding, D. B., "The Numerical Computation of Turbulent Flows," *Computational Methods in Applied Mechanical Engineering*, Vol. 3, 1974, pp. 269–289.

[21]Reynolds, W. C., "Fundamentals of Turbulence for Turbulence Modeling and Simulation," *Lecture Notes for Von Kármán Institute*, AGARD Lecture Series No. 86, 1987, pp. 1–66.

[22]Speziale, C. G., "Analytical Methods for the Development of Reynolds-Stress Closures in Turbulence," *Annual Review of Fluid Mechanics*, Vol. 23, 1991, pp. 107–157.

[23]Rodi, W., "A New Algebraic Relation for Calculating the Reynolds Stresses," *ZAMM*, Vol. 56, 1976, pp. T219–T221.

[24]Speziale, C. G., Sarkar, S., and Gatski, T. B., "Modeling the Pressure–Strain Correlation of Turbulence: An Invariant Dynamical Systems Approach," *Journal of Fluid Mechanics*, Vol. 227, 1991, pp. 245–272.

[25]Pope, S. B., "A More General Effective Viscosity Hypothesis," *Journal of Fluid Mechanics*, Vol. 72, 1975, pp. 331–340.

[26]Gatski, T. B., and Speziale, C. G., "On Explicit Algebraic Stress Models for Complex Turbulent Flows," *Journal of Fluid Mechanics*, Vol. 254, 1993, pp. 59–78.

[27]Speziale, C. G., and Xu, X. H., "Towards the Development of Second-Order Closure Models for Non-Equilibrium Turbulent Flows," *International Journal of Heat and Fluid Flow*, Vol. 17, No. 3, 1996, pp. 238–244.

[28]Abid, R., Morrison, J. H., Gatski, T. B., and Speziale, C. G., "Prediction of Aerodynamic Flows with a New Explicit Algebraic Stress Model," *AIAA Journal*, Vol. 34, No. 12, 1996, pp. 2632–2635.

[29]Speziale, C. G., "Modeling of Turbulent Transport Equations," *Simulation and Modeling of Turbulent Flows*, edited by T. B. Gatski, M. Y. Hussaini, and J. L. Lumley, Oxford Univ. Press, Oxford, England, UK, 1996, pp. 185–242.

[30]Daly, B. J., and Harlow, F. H., "Transport Equations in Turbulence," *Physics of Fluids*, Vol. 13, 1970, pp. 2634–2649.

[31]Hanjalic, K., and Launder, B. E., "A Reynolds Stress Model of Turbulence and its Application to Thin Shear Flows," *Journal of Fluid Mechanics*, Vol. 52, 1972, pp. 609–638.

[32]Mellor, G. L., and Herring, H. J., "A Survey of Mean Turbulent Field Closure Models," *AIAA Journal*, Vol. 11, No. 5, 1973, pp. 590–599.

[33]Launder, B. E., Reece, G. J., and Rodi, W., "Progress in the Development of a Reynolds Stress Turbulence Closure," *Journal of Fluid Mechanics*, Vol. 68, 1975, pp. 537–566.

[34]Gibson, M. M., and Launder, B. E., "Ground Effects on Pressure Fluctuations in the Atmospheric Boundary Layer," *Journal of Fluid Mechanics*, Vol. 86, 1978, pp. 491–511.

[35]Rotta, J. C., "Recent Attempts to Develop a Generally Applicable Calculation Method for Turbulent Shear Flow Layers," AGARD-CP-93, 1972.

[36]Abid, R., and Speziale, C. G., "Predicting Equilibrium States with Reynolds Stress Closures in Channel Flow and Homogeneous Shear Flow," *Physics of Fluids A*, Vol. 5, 1993, pp. 1776–1782.

[37]Tavoularis, S., and Karnik, U., "Further Experiments on the Evolution of Turbulent Stresses and Scales in Uniformly Sheared Turbulence," *Journal of Fluid Mechanics*, Vol. 204, 1989, pp. 457–478.

[38]Rogers, M. M., "The Structure of a Passive Scalar Field with a Uniform Mean Gradient in Rapidly Sheared Homogeneous Turbulent Flow," *Physics of Fluids A*, Vol. 3, 1991, pp. 144–154.

[39]Lee, M. J., Kim, J., and Moin, P., "Structure of Turbulence at High Shear Rate," *Journal of Fluid Mechanics*, Vol. 216, 1990, pp. 561–583.

[40]Saffman, P. G., "Results of a Two-Equation Model for Turbulent Flows and Development of a Relaxation Stress Model for Application to Straining and Rotating Flows," *Proceedings of Project SQUID Workshop on Turbulence in Internal Flows*, edited by S. Murthy, Hemisphere, New York, 1977, pp. 191–231.

[41]Speziale, C. G., and Abid, R., "Near-Wall Integration of Reynolds Stress Turbulence Closures with No Wall Damping," *AIAA Journal*, Vol. 33, No. 10, 1995, pp. 1974–1977.

[42]Orszag, S. A., Staroselsky, I., and Yakhot, V., "Some Basic Challenges for Large-Eddy Simulation Research," *Large-Eddy Simulation of Complex Engineering and Geophysical Flows*, edited by B. Galperin and S. A. Orszag, Cambridge Univ. Press, New York, 1993, pp. 237–374.

[43]Speziale, C. G., Abid, R., and Blaisdell, G. A., "On the Consistency of Reynolds Stress Turbulence Closures with Hydrodynamic Stability Theory," *Physics of Fluids*, Vol. 8, 1996, pp. 781–788.

[44]Speziale, C. G., "On Nonlinear K–ℓ and K–ε Models of Turbulence," *Journal of Fluid Mechanics*, Vol. 178, pp. 459–475.

[45]Yoshizawa, A., "Statistical Analysis of the Deviation of the Reynolds Stress from its Eddy Viscosity Representation," *Physics of Fluids*, Vol. 27, pp. 1377–1387.

[46]Rubinstein, R., and Barton, J. M., "Nonlinear Reynolds Stress Models and the Renormalization Group," *Physics of Fluids A*, Vol. 2, pp. 1472–1476.

[47]Kim, J., Kline, S. J., and Johnston, J. P., "Investigation of a Reattaching Turbulent Shear Layer: Flow Over a Backward Facing Step," *Journal of Fluids Engineering*, Vol. 102, 1980, pp. 302–308.

[48]Eaton, J. K., and Johnston, J. P., "Turbulent Flow Reattachment: An Experimental Study of the Flow and Structure Behind a Backward Facing Step," Dept. of Mechanical Engineering, TR MD-39, Stanford Univ., Stanford, CA, June 1980.

[49]Speziale, C. G., and Ngo, T., "Numerical Solution of Turbulent Flow Past a Backward Facing Step Using a Nonlinear K–ε Model," *International Journal of Engineering Science*, Vol. 26, 1988, pp. 1099–1112.

[50]Wieghardt, K., and Tillman, W., "On the Turbulent Friction Layer for Rising Pressure," NACA TM 1314, Oct. 1951.

[51]Speziale, C. G., Abid, R., and Anderson, E. C., "Critical Evaluation of Two-Equation Models for Near-Wall Turbulence," *AIAA Journal*, Vol. 30, No. 2, 1992, pp. 324–331.

[52]Schmitt, V., and Charpin, F., "Pressure Distribution on the ONERA M6 Wing at Transonic Mach Numbers," AGARD-AR-138, May 1979.

G. M. Faeth
Associate Editor